

Hybrid NRG-DMRG approach to real-time dynamics of quantum impurity systems

Fabian Güttge,¹ Frithjof B. Anders,¹ Ulrich Schollwöck,² Eitan Eidelstein,^{3,4} and Avraham Schiller³

¹*Lehrstuhl für Theoretische Physik II, Technische Universität Dortmund, 44221 Dortmund, Germany*

²*Physics Department, Arnold Sommerfeld Center for Theoretical Physics, and Center for NanoScience, Ludwig-Maximilians-Universität München, D-80333 München, Germany*

³*Racah Institute of Physics, The Hebrew University, Jerusalem 91904, Israel*

⁴*Department of Physics, NRCN, P.O. Box 9001, Beer-Sheva, 84190 Israel*

A hybrid approach to nonequilibrium dynamics of quantum impurity systems is presented. The numerical renormalization group serves as a means to generate a suitable low-energy Hamiltonian, allowing for an accurate evaluation of the real-time dynamics of the problem up to exponentially long times using primarily the time-adaptive density-matrix renormalization group. We extract the decay time of the interaction-enhanced oscillations in the interacting resonant-level model and show their quadratic divergence with the interaction strength U . Our numerical analysis is in excellent agreement with analytic predictions based on an expansion in $1/U$.

PACS numbers: 73.21.La, 73.63.Rt, 72.15.Qm

Introduction. The description of strong electronic correlations far from thermal equilibrium poses an enormous theoretical challenge. At the root of the problem lies the nonequilibrium density operator which is not explicitly known in the presence of interactions. Of particular relevance are quench and driven dynamics realized in pump-probe experiments [1, 2], atomic traps [3, 4], and nanodevices [5, 6], where the full time evolution of the density operator should, in principle, be tracked.

Quantum impurities systems (QIS) have regained considerable attention over the past 15 years due to the advent of carefully designed nanodevices. These generically consist of a few locally interacting degrees of freedom, typically a quantum dot, in contact with macroscopic leads. Since driven dynamics in nanodevices is of practical relevance to quantum computing and quantum control, considerable efforts were mounted in recent years toward devising approaches capable of treating the nonequilibrium state in QIS.

Significant analytical progress in the calculation of real-time dynamics was achieved using different adaptations of perturbative renormalization-group ideas [7–9]. However, with the exception of Ref. [10], these are confined to the weak-coupling regime. Numerical methods, such as applications of the time-dependent density-matrix renormalization group (TD-DMRG) [11, 12] to QIS [13, 14], the time-dependent numerical renormalization group (TD-NRG) [15], an iterated path-integral approach [16], and different continuous-time Monte Carlo simulations [17–19], are more flexible in the parameter regimes they can treat, but are either restricted to short time scales [13, 14, 16–19] or susceptible to finite-size and discretization errors [13–15]. Indeed, finite-size representations are faced with an inherent difficulty of accurately representing the continuum limit even on intermediate time scales.

In this paper, we report the extension of a recent hybrid approach [20] that overcomes some of the major ob-

stacles hampering the description of quench dynamics in QIS. The basic idea is to exploit the outstanding capabilities of the TD-NRG to bridge over vastly different time scales in order to systematically construct an effective low-energy Hamiltonian, whose real-time dynamics can be calculated using complementary approaches that do not rely on the special structure of the Wilson chain. In this manner, one can largely eliminate discretization errors inherent to the Wilson chain while boosting the complementary approach to times scales orders of magnitude beyond its natural capabilities. As a proof of principle, we have hybridized in Ref. [20] the TD-NRG with the Chebyshev expansion technique (CET) [21]. In this paper, we demonstrate the full power of the approach by hybridizing the TD-NRG with the TD-DMRG [12].

Focusing on the interacting resonant-level model (IRLM) [22, 23], we show that one can essentially eliminate discretization errors on all time scales of interest by constructing a suitable hybrid chain. This, in turn, allows for a thorough examination of the interaction-enhanced oscillations first reported in Ref. [20], yielding excellent agreement with analytical predictions for their frequency and damping time. The latter is shown to diverge quadratically with the interaction strength, demonstrating that relaxation to equilibrium can involve new time scales far longer than the thermodynamic ones.

Hybrid-NRG. We begin with a concise derivation of the hybrid-NRG [20]. The Hamiltonian $\mathcal{H} = \mathcal{H}_{\text{bath}} + \mathcal{H}_{\text{imp}} + \mathcal{H}_{\text{mix}}$ of a quantum impurity problem consists of three parts: $\mathcal{H}_{\text{bath}}$ models the continuous bath, \mathcal{H}_{imp} represents the decoupled impurity, and \mathcal{H}_{mix} describes the coupling between the two subsystems. For $t < 0$, the entire system is assumed to be characterized by a density operator $\hat{\rho}_0$ associated with an initial Hamiltonian \mathcal{H}^i . Specifically, $\hat{\rho}_0$ can either be the equilibrium density operator corresponding to \mathcal{H}^i , or may project onto one of its low-lying eigenstates, typically the ground state. At time $t = 0$, a static perturbation is abruptly switched

on such that $\mathcal{H}^i \rightarrow \mathcal{H}^f$. Our goal is to track the time evolution of local expectation values: $O(t) = \text{Tr}\{\hat{\rho}(t)\hat{O}\}$ with $\hat{\rho}(t) = e^{-it\mathcal{H}^f}\hat{\rho}_0 e^{it\mathcal{H}^f}$.

In Wilson's numerical renormalization group (NRG) [24], $\mathcal{H}_{\text{bath}}$ is discretized logarithmically using a dimensionless parameter $\Lambda > 1$, and mapped onto a semi-infinite chain whose open end is coupled to the impurity via \mathcal{H}_{mix} . Wilson's chain is characterized by exponentially decreasing hopping matrix elements $t_m \propto D\Lambda^{-m/2}$, defining a natural separation of scales. This enables an iterative diagonalization of \mathcal{H} , where at each step only the lowest N_s eigenstates are retained. Terminating the procedure after N steps, the collection of states discarded after each iteration combine to form a complete basis set of approximate NRG eigenstates of \mathcal{H} on the N -site chain [15]. The expectation value of any local operator \hat{O} can be formally expressed as [15]

$$O(t \geq 0) = \sum_{m=0}^N \sum_{r,s}^{\text{trun}} O_{r,s}^m \rho_{s,r}^m(t), \quad (1)$$

where r and s run over the NRG eigenstates of \mathcal{H}^f at iteration $m \leq N$, $O_{r,s}^m$ is the matrix representation of \hat{O} at that iteration, and $\rho_{s,r}^m(t)$ is the corresponding time-dependent reduced density matrix. The restricted sum over r and s requires that at least one of these states is discarded at iteration m .

Partitioning the sum over m into $m \leq M$ and $M < m$ at some arbitrary but fixed $M < N$, Eq. (1) is recast as

$$O(t \geq 0) = \sum_{m=0}^M \sum_{r,s}^{\text{trun}} O_{r,s}^m \rho_{s,r}^m(t) + \text{Tr}\{\hat{1}_M^+ \hat{O} \hat{1}_M^+ \hat{\rho}(t) \hat{1}_M^+\}, \quad (2)$$

where $\hat{1}_M^+$ projects onto the subspace retained at the conclusion of iteration M . Equation (2) is formally exact, relying solely on the completeness of our basis set [15]. It has the following interpretation. At each energy scale $D\Lambda^{-m/2}$ with $m \leq M$, only those terms involving at least one discarded high-energy state contribute to $O(t)$, leaving the contribution of the low-energy subspace retained at the conclusion of iteration M . In the process, the NRG has produced an effective quantum-impurity Hamiltonian \mathcal{H}_{M+1} with the reduced bandwidth $D_{\text{eff}} \propto D\Lambda^{-M/2}$:

$$\begin{aligned} \mathcal{H}_{M+1} = & \sum_k E_k^M |k; M\rangle \langle k; M| \\ & + \sum_{m=M}^{N-1} \sum_{\nu} t_m \hat{1}_M^+ \{f_{m+1,\nu}^\dagger f_{m,\nu} + \text{H.c.}\} \hat{1}_M^+. \end{aligned} \quad (3)$$

Here, $f_{m,\nu}^\dagger$ creates an electron of flavor (spin) ν on the chain site m , $|k; M\rangle$ labels the kept NRG eigenstates at iteration M , and E_k^M are the corresponding NRG eigenenergies. Usually, one would proceed with the NRG to iteratively diagonalize \mathcal{H}_{M+1} . Here, we follow a different route: (i) we abandon the traditional Wilson

chain and seek an optimal choice for the hopping amplitudes t_m with $m \geq M$; (ii) \mathcal{H}_{M+1} is used as input for our complementary method of choice in order to compute $\text{Tr}\{\hat{1}_M^+ \hat{O} \hat{1}_M^+ \hat{\rho}(t) \hat{1}_M^+\}$; (iii) employing the standard NRG approximation $\rho_{s,r}^m(t) \approx e^{i(E_r^m - E_s^m)t} \rho_{s,r}^{\text{red}}(m)$ [15], $\rho_{s,r}^{\text{red}}(M)$ as produced by our method of choice is feed back into the TD-NRG to account for the remaining high-energy dynamics in Eq. (2).

In this paper, we supplement the TD-NRG with the adaptive TD-DMRG [12]. The system is assumed to initially occupy the ground state $|\psi_0\rangle$ of \mathcal{H}_{M+1}^i , constructed using the DMRG [25]. Accordingly, $\hat{\rho}(t)$ equals $|\psi(t)\rangle \langle \psi(t)|$ with $|\psi(t)\rangle = e^{-it\mathcal{H}^f} |\psi_0\rangle$, resulting in $\text{Tr}\{\hat{1}_M^+ \hat{O} \hat{1}_M^+ \hat{\rho}(t) \hat{1}_M^+\} = \langle \chi_M(t) | \hat{O} | \chi_M(t) \rangle$. Here $|\chi_M(t)\rangle = \hat{1}_M^+ |\psi(t)\rangle$ is the projection of $|\psi(t)\rangle$ onto the low-energy subspace retained at the conclusion of iteration M . Although Eq. (2) is formally exact for arbitrary M , the larger is $N_\chi = \langle \chi_M(t) | \chi_M(t) \rangle \leq 1$ the smaller is the contribution of the sum on the right-hand side of Eq. (2). If $(1 - N_\chi) < \epsilon$ for some small number ϵ , then $|\chi_M(t)\rangle = |\psi(t)\rangle + \mathcal{O}(\sqrt{\epsilon})$, and the major contribution to the real-time dynamics originates from $\langle \chi_M(t) | \hat{O} | \chi_M(t) \rangle$.

A proper choice of M is important. Initially, the NRG level flows [24] of \mathcal{H}^i and \mathcal{H}^f are nearly identical. We choose M to be a characteristic iteration after which the two level flows begin to significantly deviate from one another [15, 24]. The corresponding energy scale, $D\Lambda^{-M/2}$, is typically of order the energy difference between \mathcal{H}^i and \mathcal{H}^f . By that choice of M , the major contribution to $O(t)$ stems from $\langle \chi_M(t) | \hat{O} | \chi_M(t) \rangle$. We approximate $|\chi_M(t)\rangle$ by $\exp(-i\mathcal{H}_{M+1}^f t) \hat{1}_M^+ |\psi_0\rangle$, adopting the NRG philosophy that excitations on different energy scales are only weakly coupled [20]. Thus, the NRG generates a suitable low-energy Hamiltonian, allowing for the real-time dynamics of the problem to be explored on the exponentially long time scale $1/D_{\text{eff}} \propto \Lambda^{M/2}$ using mainly the TD-DMRG.

The model. We shall demonstrate our hybrid NRG-DMRG approach by investigating the quench dynamics in the IRLM, defined by the Hamiltonian

$$\begin{aligned} \mathcal{H} = & \sum_k \epsilon_k c_k^\dagger c_k + E_d d^\dagger d + \frac{V}{\sqrt{N_k}} \sum_k \{c_k^\dagger d + \text{H.c.}\} \\ & + \frac{U}{N_k} \sum_{k,k'} :c_k^\dagger c_{k'} : \left(d^\dagger d - \frac{1}{2} \right). \end{aligned} \quad (4)$$

Here, d^\dagger creates an electron on the impurity level, c_k^\dagger creates a band electron with momentum k , N_k denotes the number of distinct k points, and $:c_k^\dagger c_{k'} : := c_k^\dagger c_{k'} - \delta_{k,k'} \theta(-\epsilon_k)$ stands for normal ordering with respect to the filled Fermi sea. The basic energy scales in the problem include the level energy E_d and the hybridization width $\Gamma_0 = \pi \varrho V^2$, where ϱ is the conduction-electron density of states at the Fermi energy. The effect of the contact interaction is to renormalize the hybridization width at resonance according to $\Gamma_0 \rightarrow \Gamma_{\text{eff}} \approx D(\Gamma_0/D)^{1/(1+\alpha)}$,

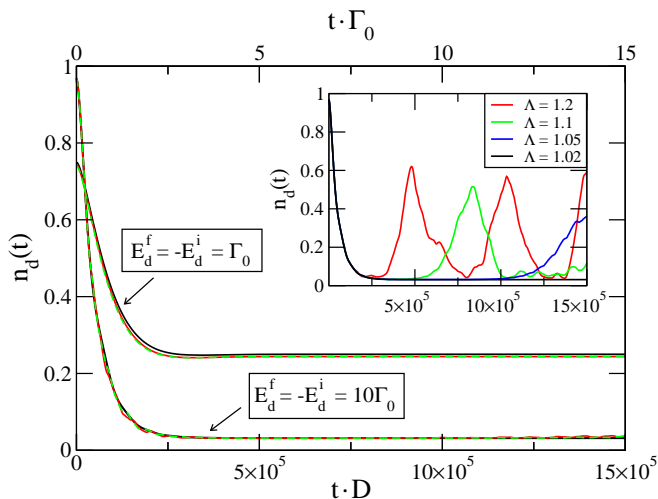


FIG. 1. (Color online) Time evolution of $n_d(t)$ on a double Wilson chain, following a sudden change of the level energy from E_d^i to E_d^f . Here $\Gamma_0/D = 10^{-5}$ and $U = 0$. The full red line depicts the exact solution on the double Wilson chain (obtained by exact diagonalization), the dashed green line displays the hybrid NRG-DMRG, and the full black line is the exact analytical continuum-limit solution [15] in the wide-band limit. Chain parameters: $M = 29$, $\Lambda_1 = 1.8$, $\Lambda_2 = 1.02$, $N_{\text{inter}} = 4$, and $N = 180$. $N_s = 50$ states are retained both in the NRG and in the course of the TD-DMRG. Inset: Exact $n_d(t)$ on a pure Wilson chain, for $E_d^f = -E_d^i = 10\Gamma_0$ and different Λ 's. Here $N = 500$ (1000) for $\Lambda \geq 1.1$ ($\Lambda \leq 1.05$).

with $\alpha = 2\delta - \delta^2$ and $\delta = (2/\pi) \arctan(\pi\rho U/2)$ (D is the bandwidth). Although the thermodynamics of the IRLM was investigated over 30 years ago [22, 23], there has been a recent surge of interest in its nonequilibrium properties, particularly for a biased two-lead setting [7, 9, 26, 27]. Focusing on the single-band version of Eq. (4), we consider an abrupt shift of the level energy at time $t = 0$ from E_d^i to E_d^f , with the goal of tracking the time evolution of the level occupancy, $n_d(t) = \langle \hat{d}^\dagger(t)\hat{d}(t) \rangle$.

Hybrid chain. There are two sources of deviations from the continuum limit when considering quench dynamics on a pure Wilson chain: (i) internal reflections of currents caused by the exponentially decreasing hopping matrix elements along the chain [20, 28] (leading, in turn, to an exponential slowing down of the transport velocity); (ii) reflections at the end of the finite-size chain that propagate back to the impurity. While the former source of error is eliminated for an ordinary tight-binding chain, the latter point is unavoidable in nearly all practical calculations as the total chain length is limited by computational demands. Thus, one would like to simultaneously minimize the internal reflections and the transport velocity down the chain to accurately access long times.

Guided by these considerations, we found it advantageous to use a double Wilson chain, constructed by patching two separate Wilson chains. The first M hopping matrix elements t_m with $0 \leq m \leq M - 1$ are taken

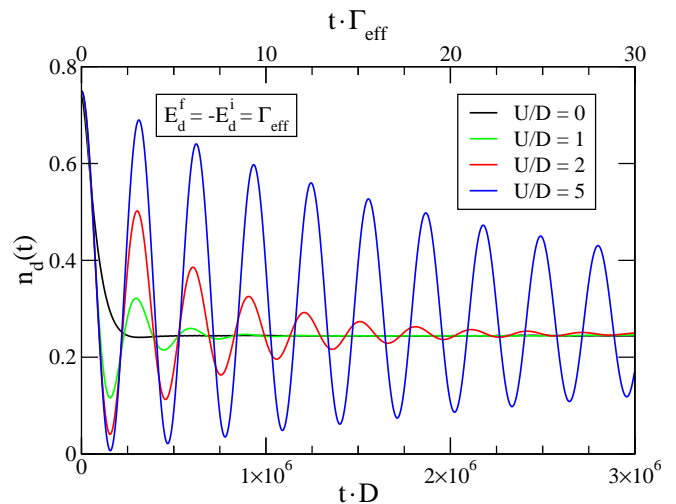


FIG. 2. (Color online) Same as Fig. 1, for $E_d^f = -E_d^i = \Gamma_{\text{eff}}$ and different values of U . Γ_0 was adjusted separately for each value of U so as to maintain $\Gamma_{\text{eff}}/D = 10^{-5}$. All other chain, NRG, and TD-DMRG parameters are the same as in Fig. 1.

to be the customary Wilson hopping amplitudes [24] with the discretization parameter Λ_1 . Further down the chain a second, smaller discretization parameter Λ_2 is used, with a magnitude close to but larger than one [30]. To reduce internal reflections, the transition from Λ_1 to Λ_2 is smoothed according to $t_{M+m} = \lambda_m^{-1/2} t_{M+m-1}$ with

$$\lambda_m = \begin{cases} \Lambda_1 - \frac{\Lambda_1 - \Lambda_2}{N_{\text{inter}}}(m + 1), & 0 \leq m < N_{\text{inter}}, \\ \Lambda_2, & N_{\text{inter}} \leq m. \end{cases} \quad (5)$$

Results. The merit of such a double Wilson chain is demonstrated in Fig. 1, where $n_d(t)$ is plotted following a quench from E_d^i to E_d^f . The interaction U is set to zero, to facilitate comparison with an exact continuum-limit solution in the wide-band limit [15], as well as with an exact numerical solution on the hybrid chain, obtained by exact diagonalization of the single-particle eigenmodes. We set $\Gamma_0/D = 10^{-5}$, placing the basic time scale $1/\Gamma_0$ orders of magnitude beyond the reach of pure TD-DMRG. The parameter M was chosen such that $D\Lambda_1^{-M/2} \approx 20\Gamma_0$ is twice the maximal value of $|E_d|$ used.

Evidently, deviations between the continuum limit, the exact solution on the hybrid chain, and the hybrid NRG-DMRG approach are hardly discernible up to long time scales, well after the occupancy has relaxed to its new equilibrium value. For $E_d^f = -E_d^i = \Gamma_0$, the excellent agreement persists up to $t \gtrsim 30/\Gamma_0$, at which point all three curves begin to separate. For $E_d^f = -E_d^i = 10\Gamma_0$, the agreement extends up to slightly above $15/\Gamma_0$. As analyzed in the inset, an impractically small discretization parameter $\Lambda \approx \Lambda_2 = 1.02$ is needed to achieve a comparable representation of the continuum limit using a pure Wilson chain.

In Fig. 2, we analyze the effect of a finite U on $n_d(t)$.

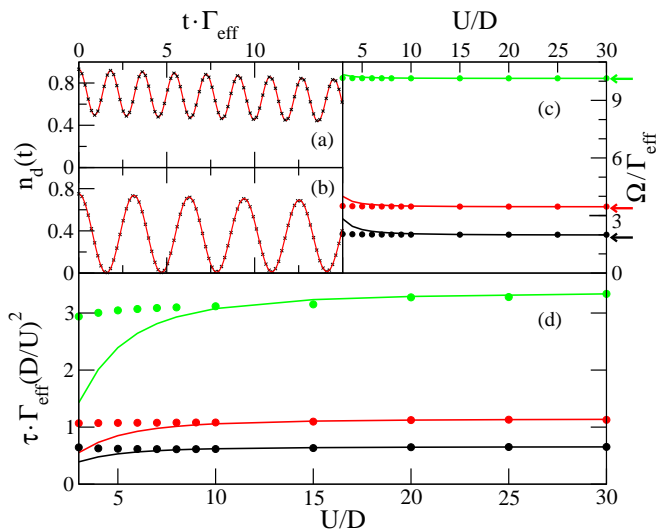


FIG. 3. (Color online) (a) Interaction-enhanced oscillations (red line) for $E_d^f = -E_d^i = 3\Gamma_{\text{eff}}$ and $U/D = 10$, along with a fit to Eq. (7) (black crosses). (b) Same as (a), for $E_d^f = -E_d^i = \Gamma_{\text{eff}}$. (c) The fitted frequency Ω vs U for $E_d^f/\Gamma_{\text{eff}} = -E_d^i/\Gamma_{\text{eff}} = 1$ (black circles), 3 (red circles), and 10 (green circles). Full lines display the analytical strong-coupling expression for Ω , employing the numerical values of V . Arrows on the right-hand side mark the asymptotic $U \rightarrow \infty$ values of Ω . (d) Same as (c) for the decay time τ . All remaining parameters are the same as in Fig. 2.

At low energies, the IRLM is equivalent to its noninteracting counterpart, both describing a phase-shifted Fermi liquid. Near resonance, the effect of U in equilibrium is to renormalize Γ_0 to Γ_{eff} , hence one may expect $n_d(t)$ to follow the same curves as in Fig. 1 upon substituting $\Gamma_0 \rightarrow \Gamma_{\text{eff}}$. This, however, is not the case. In Fig. 2 we adjusted Γ_0 separately for each value of U so as to maintain a fixed $\Gamma_{\text{eff}}/D = 10^{-5}$. To this end, we fixed $E_d/D = -10^{-5}$ and scanned Γ_0 using the hybrid NRG-DMRG until a ground-state occupancy of $n_d = 0.75$ was reached. As first reported in Ref. [20], interaction-enhanced oscillations gradually develop in $n_d(t)$ upon increasing U . For large U , exemplified by $U/D = 5$, these oscillations decay on a time scale much longer than $1/\Gamma_{\text{eff}}$, revealing the emergence of a new time scale unrelated to the thermodynamic ones. Note that, as for $U = 0$, our curves appear to faithfully represent the continuum limit up to $t \gtrsim 30/\Gamma_{\text{eff}}$ for this moderate quench.

The extended time scales and supreme accuracy of the hybrid NRG-DMRG allow for a detailed quantitative analysis of the interaction-enhanced oscillations, which was previously impossible using the hybrid NRG-Chebyshev approach [20]. The understanding of the interaction-enhanced oscillations employs a strong-coupling expansion in $1/U$. For $U \rightarrow \infty$, the impurity level and zeroth Wilson shell decouple from the rest of the chain, being confined to a combined valence of

one. Within this subspace, the two eigenstates of the local Hamiltonian have the energies $\epsilon_{\pm} = (E_d/2) \pm \sqrt{(E_d/2)^2 + V^2}$, hence $n_d(t)$ displays quantum beats with the frequency $\Omega = \epsilon_+ - \epsilon_- = 2\sqrt{(E_d/2)^2 + V^2}$ [20]. For large but finite U , the coherent oscillations are damped by the residual coupling to the rest of the chain, which introduces a finite lifetime of the state ϵ_+ . We expand to order $1/U$ about the $U \rightarrow \infty$ limit, which yields the residual coupling to the rest of the chain. Using Fermi's golden rule, the decay time is found to be

$$\tau^{-1} = \pi \left(\frac{8D}{\pi^2 U} \right)^2 \frac{V^2}{\sqrt{(E_d/2)^2 + V^2}}. \quad (6)$$

Further neglecting rearrangements of the bath electrons (themselves being controlled by $1/U$), we deduce the functional form

$$n_d(t) = A \left[e^{-t/2\tau} \cos(\Omega t) \sqrt{1 - e^{-t/\tau} \cos^2 \theta} - e^{-t/\tau} \sin \theta \right] + n_{\text{eq}} \left(1 - e^{-t/\tau} \right) + n_d(0) e^{-t/\tau}, \quad (7)$$

where n_{eq} is the equilibrated long-time occupancy, while A and θ have no direct relation to any simple observable.

Panels (a) and (b) of Fig. 3 show typical fits of $n_d(t)$ to Eq. (7), using τ , Ω , A , θ , and $n_d(0) = 1 - n_{\text{eq}}$ as fitting parameters. The fitting range, $t \cdot \Gamma_{\text{eff}} \leq 10$, was carefully chosen to exclude any discretization error. Evidently, Eq. (7) well describes the numerical curves, further validating the expansion in $1/U$. The extracted values of Ω and τ , plotted in panels (c) and (d) for different quenches, practically coincide above $U/D \approx 10$ with the analytical predictions, confirming, in particular, that $\tau \propto U^2$.

Summary. A new hybrid NRG-DMRG approach was devised that largely eliminates discretization errors hampering the TD-NRG, while boosting the TD-DMRG to time scales orders of magnitude beyond its natural reach. The approach allows access to exceptionally long times with unparallel accuracy, as demonstrated by a detailed analysis of the interaction-enhanced oscillations in the IRLM. These outstanding capabilities open the door, so we hope, to accurate investigations of systems and coupling regimes that so far remained well beyond reach.

Acknowledgments This work was supported by the German-Israeli Foundation through grant no. 1035-36.14, and by the Deutsche Forschungsgemeinschaft under AN 275/6-2 (F.G. and F.B.A.).

-
- [1] L. Perfetti, P. A. Loukakos, M. Lisowski, U. Bovensiepen, H. Berger, S. Biermann, P. S. Cornaglia, A. Georges, and M. Wolf, Phys. Rev. Lett. **97**, 067402 (2006).
 - [2] F. Schmitt, P. S. Kirchmann, U. Bovensiepen, R. G. Moore, L. Rettig, M. Krenz, J.-H. Chu, N. Ru, L. Perfetti, D. H. Lu, M. Wolf, I. R. Fisher, and Z.-X. Shen, Science **321**, 1649 (2008).

- [3] M. Greiner, O. Mandel, T. W. Hänsch, and I. Bloch, *Nature* **419**, 51 (2002); T. Kinoshita, T. Wenger, and D. S. Weiss, *Nature* **440**, 900 (2006).
- [4] S. Trotzky, Y.-A. Chen, A. Flesch, I. P. McCulloch, U. Schollwöck, J. Eisert, and I. Bloch, *Nature Physics* **8**, 325 (2012).
- [5] J. M. Elzerman, R. Hanson, L. H. W. van Beveren, B. Witkamp, L. M. K. Vandersypen, and L. P. Kouwenhoven, *Nature* **430**, 431 (2004).
- [6] J. R. Petta, A. C. Johnson, J. M. Taylor, E. A. Laird, A. Yacoby, M. D. Lukin, C. M. Marcus, M. P. Hanson, and A. C. Gossard, *Science* **309**, 2180 (2005).
- [7] M. Pletyukhov, D. Schuricht, and H. Schoeller, *Phys. Rev. Lett.* **104**, 106801 (2010); S. Andergassen, M. Pletyukhov, D. Schuricht, H. Schoeller, and L. Borda, *Phys. Rev. B* **83**, 205103 (2011); C. Karrasch, S. Andergassen, M. Pletyukhov, D. Schuricht, L. Borda, V. Meden, and H. Schoeller, *Europhys. Lett.* **90**, 30003 (2010).
- [8] A. Hackl and S. Kehrein, *J. Phys. C* **21**, 015601 (2009); A. Hackl, M. Vojta, and S. Kehrein, *Phys. Rev. B* **80**, 195117 (2009); P. Wang and S. Kehrein, *Phys. Rev. B* **82**, 125124 (2010).
- [9] D. M. Kennes, S. G. Jakobs, C. Karrasch, and V. Meden, Report no. arXiv:1111.6982.
- [10] M. Pletyukhov and H. Schoeller, Report no. arXiv:1201.6295.
- [11] G. Vidal, *Phys. Rev. Lett.* **93**, 040502 (2004); A. J. Daley, C. Kollath, U. Schollwöck, and G. Vidal, *J. Stat. Mech.: Theor. Exp.* P04005 (2004); S. R. White and A. E. Feiguin, *Phys. Rev. Lett.* **93**, 076401 (2004).
- [12] For a recent review on the DMRG and TD-DMRG, see U. Schollwöck, *Ann. Phys.* **326**, 96 (2011).
- [13] P. Schmitteckert, *Phys. Rev. B* **70**, 121302 (2004); A. Branschaedel, G. Schneider, and P. Schmitteckert, *Ann. Phys.* **522**, 657 (2010).
- [14] K. A. Al-Hassanieh, A. E. Feiguin, J. A. Riera, C. A. Büsser, and E. Dagotto, *Phys. Rev. B* **73**, 195304 (2006); L. G. G. V. Dias da Silva, F. Heidrich-Meisner, A. E. Feiguin, C. A. Büsser, G. B. Martins, E. V. Anda, and E. Dagotto, *Phys. Rev. B* **78**, 195317 (2008); F. Heidrich-Meisner, A. E. Feiguin, and E. Dagotto, *Phys. Rev. B* **79**, 235336 (2009).
- [15] F. B. Anders and A. Schiller, *Phys. Rev. Lett.* **95**, 196801 (2005); *Phys. Rev. B* **74**, 245113 (2006).
- [16] S. Weiss, J. Eckel, M. Thorwart, and R. Egger, *Phys. Rev. B* **77**, 195316 (2008).
- [17] L. Mühlbacher and E. Rabani, *Phys. Rev. Lett.* **100**, 176403 (2008).
- [18] P. Werner, T. Oka, and A. J. Millis, *Phys. Rev. B* **79**, 035320 (2009); P. Werner, T. Oka, M. Eckstein, and A. J. Millis, *Phys. Rev. B* **81**, 035108 (2010).
- [19] M. Schiró and M. Fabrizio, *Phys. Rev. B* **79**, 153302 (2009).
- [20] E. Eidelstein, A. Schiller, F. Güttge, and F. B. Anders, *Phys. Rev. B* **85**, 075118 (2012).
- [21] H. Tal Ezer and R. Kosloff, *J. Chem. Phys.* **81**, 3967 (1984).
- [22] P. W. Vigman and A. M. Finkelstein, *Zh. Eksp. Theor. Fiz.* **75**, 204 (1978) [*Sov. Phys. JETP* **48**, 102 (1978)].
- [23] P. Schlottmann, *Phys. Rev. B* **22**, 622 (1980).
- [24] K. G. Wilson, *Rev. Mod. Phys.* **47**, 773 (1975); R. Bulla, T. A. Costi, and T. Pruschke, *Rev. Mod. Phys.* **80**, 395 (2008).
- [25] S. R. White, *Phys. Rev. Lett.* **69**, 2863 (1992); *Phys. Rev. B* **48**, 10345 (1993).
- [26] P. Mehta and N. Andrei, *Phys. Rev. Lett.* **96**, 216802 (2006).
- [27] E. Boulat, H. Saleur, and P. Schmitteckert, *Phys. Rev. Lett.* **101**, 140601 (2008).
- [28] P. Schmitteckert, *J. Phys.: Conference Series* **220**, 012022 (2010).
- [29] A. Weichselbaum, F. Verstraete, U. Schollwöck, J. I. Cirac, and Jan von Delft, *Phys. Rev. B* **80**, 165117 (2009).
- [30] Another motivation for using a modified Wilson chain was recently given in Ref. [29]. These authors adopted a different point of view and a different construction based upon Wilson's original discretization of the bath.